Optical Engineering

SPIEDigitalLibrary.org/oe

Combination method of digital holography and gravimetric measurement for assessment of a paint drying process

Masayuki Yokota
Yoshiki Kimoto

SPIE

Combination method of digital holography and gravimetric measurement for assessment of a paint drying process

Masayuki Yokota
Yoshiki Kimoto
Shimane University
Department of Mechanical, Electrical and Electronic Engineering
Shimane, Japan
E-mail: yokota@ecs.shimane-u.ac.jp

Abstract. A combination method to study the drying process of paints, based on digital holography and gravimetric measurement, is proposed. The proposed method allows taking holographic measurement in a simultaneous way to compare the results obtained by the reconstructed image changes with gravimetric data. By directly comparing a phase change in the reconstructed images of a paint surface and weight change of the paint film, it is found that a stationary state of the paint surface detected by the phase change occurs in the last stage of solvent evaporation and corresponds to a dry-hard of the paint film. The proposed technique can also analyze dryness of clear coat having no scattering particle using the phase change. It is shown that the present technique can allow us to further investigate not only a film formation of clear coat but also an estimation of specific gravity of solvents by comparing directly the phase change with weight loss due to solvent evaporation in the simultaneous measurement. [DOI: 10.1117/1.OE.52.1.015801]

Subject terms: digital holography; gravimetric measurement; microscopic observation; paint drying process; clear coat; specific gravity; dry-hard.

Paper 121170 received Aug. 13, 2012; revised manuscript received Nov. 29, 2012; accepted for publication Dec. 4, 2012; published online Jan. 4, 2013.

1 Introduction

Painting or coating with thin layers of paint has been required in many industrial products.[1] In the coating or painting process of the products, a drying process plays an important role for their quality or productivity. Thus, the knowledge of the drying process of coatings and paints becomes highly important in the industry. For example, the evaluation of dryness of color ink is also required to determine a suitable content for high-quality printing with an inkjet printer.

For a noncontact and quantitative evaluation of paint drying process, a method using a dynamic speckle related to a variation of paint film has been studied.[2–7] The method based on a dynamic speckle interferometry has been applied to investigate the drying process of several kinds of paints. In the method, monitoring of nonuniform drying is also possible by employing an imaging system or comparing the pixel values in the successive images. However, the speckle methods have difficulties for investigation of the paint drying on a complicated three-dimensional (3-D) surface because of the necessity of scanning the imaging lens over the surfaces. Recently, lensless Fourier transform digital holography has been applied to detect a cracking/disbanding of paints.[8] In the holographic method, a quantitative analysis of dryness for 3-D paint surface has not been demonstrated.

To achieve both noncontact and quantitative analysis of paint drying on 3-D objects, we have proposed the phase-shifting digital holographic method.[9,10] It has been successfully demonstrated that a local variation of dryness of solvent-based paint can be imaged and analyzed by calculating the phase change between two subsequent reconstructed complex amplitudes of 3-D painted surfaces. We have also compared indirectly the phase change and weight loss obtained by a gravimetric measurement to investigate the relationship between an evaporation of solvent and a surface change in the last work.[10] It has been found that a stationary state of paint film detected by the phase-shifting holographic method almost corresponds to the tack-free dry of the solvent-based paint. However, the relationship between the phase variation and weight loss due to the evaporation of solvents could not be sufficiently investigated using the above indirect comparison. Therefore, direct comparison has been highly desired for further investigation of the drying process.

In this paper, we introduce the gravimetric and microscopic investigation into the holographic setup and investigate the drying process of two types of water-based paints in the simultaneous manner. A clear coat having no pigment particles is also used to investigate the applicability of holographic method to a transparent film. The specific gravity of evaporated solvent is also estimated using both the volume loss of paint film obtained from the phase change and weight loss. The sensitivity of phase in the holographic method to dryness of the paint film is studied in a direct comparison of the microscopic observation. The relationship between the evaporation rate of solvent and phase variation is further investigated by directly comparing the results of both holographic and gravimetric methods.

2 Signal Processing for Monitoring Dryness of Paint

To detect the change of wavefront reflected from the paint film in which the microscopic variation such as solvent evaporation, leveling[11] of paint film, and a movement of

0091-3286/2013/$25.00 © 2013 SPIE

pigment particles occurs, four-step temporal phase-shifting digital holography has been adopted.[12] By virtue of the phase-shifting method, the image of paint film can be obtained without the 0'th-order and conjugate images[13] and that makes the signal processing easy.

In four-step phase-shifting digital holography, we derived the complex amplitude of the object wave $U_o(x,y;t)$ at the charge coupled device (CCD) surface, which is then Fresnel transformed to reconstruct the complex amplitude $U(X,Y;t)$ at the object plane for the instance of hologram recording t.

$$\mathrm{U}(X,Y;t) = \exp\left[\frac{i\pi}{\lambda Z}(X^2+Y^2)\right] \times \int\int U_o(x,y;t)\exp\left[\frac{i\pi}{\lambda Z}(x^2+y^2)\right] \times \exp\left[-\frac{i2\pi}{\lambda Z}(xX+yY)\right]\mathrm{d}x\mathrm{d}y, \quad (1)$$

where Z is the reconstruction distance, (x,y) and (X,Y) denote the coordinates at the CCD and image planes, respectively, and λ is the wavelength of light source. The complex amplitude $U(X,Y;t)$ is digitized if the hologram $U_o(x,y;t)$ is sampled on a rectangular raster of $N\times N$ pixels, with a pixel pitch Δx and Δy of the CCD in x and y direction. For the reconstruction, a single discrete fast Fourier transform (FFT) method was conducted to fulfill the Fresnel transformation.[13] In that case, the sample interval of the reconstructed image in X and Y direction, respectively corresponds to[11]

$$\begin{cases} \Delta X = \frac{\lambda Z}{N\Delta x} \\ \Delta Y = \frac{\lambda Z}{N\Delta y} \end{cases}. \quad (2)$$

To detect a local variation of paint drying, the subsequent reconstructed complex amplitude of object wave reflected from the painted surface is obtained with an interval T and subject to the postsignal processing. The standard deviation σ_t of phase difference distribution between the successive reconstructed phases $\Delta\phi_t(X,Y) = \arg\{U(X,Y;t)U^*(X,Y;t+T)\}$ is calculated as

$$\sigma_t = \sqrt{\frac{\sum_{X,Y\in D}[\Delta\phi_t(X,Y)-\overline{\Delta\phi_t}]^2}{N_D}}, \quad (3)$$

where $\overline{\Delta\phi_t}$ is the averaged value of $\Delta\phi_t(X,Y)$ over the analyzed area D and N_D is the number of data in the area D. When the paint film is clear coat having no pigment particle, a refractive index change $\Delta n_t(X,Y)$ and a reduction of film thickness $\Delta\varepsilon_t(X,Y)$ in the two successive hologram recordings cause a change of the optical pathlength and thereby the phase difference $\Delta\phi_t(X,Y)$. So the phase difference $\Delta\phi_t(X,Y)$ can be expressed as

$$\Delta\phi_t(X,Y) = \frac{4\pi}{\lambda}\{\Delta n_t(X,Y)h_t(X,Y) + \Delta\varepsilon_t(X,Y)(n_t(X,Y)-1)\}, \quad (4)$$

where $h_t(X,Y)$ is the paint thickness and $n_t(X,Y)$ is the refractive index of the film at t. Assuming the value of $\Delta n_t(X,Y)$ to be negligibly small for the interval T, the reduction of film thickness $\Delta\varepsilon_t(X,Y)$ can be estimated from the phase difference $\Delta\phi_t(X,Y)$. The decreased volume of paint film $\Delta v(t)$ during the interval T is also calculated using

$$\Delta v(t) = \sum_{X,Y\in D}\Delta\varepsilon_t(X,Y)\Delta X\cdot\Delta Y. \quad (5)$$

By using the weight loss of paint film $\Delta M_p(t)$ obtained with the gravimetric method, the specific gravity of evaporated solvent is estimated as $d_e(t) = \Delta M_p(t)/\Delta v(t)$.

In addition, we calculated cross-correlation function $C_t(X,Y)$ between successive intensity images $I_t(X,Y) = |U(X,Y;t)|^2$ and microscopic images at two instances t and $t+T$,

$$C_t(X,Y) = \int\int I_t(X',Y')I_{t+T}(X'+X,Y'+Y)\mathrm{d}X'\mathrm{d}Y' = F^{-1}[\hat{I}_t(\xi,\eta)\hat{I}_{t+T}{}^*(\xi,\eta)], \quad (6)$$

where F^{-1} represents an inverse Fourier transform, $\hat{I}^*(\xi,\eta)$ means the complex conjugate of $\hat{I}(\xi,\eta)$, and $\hat{I}(\xi,\eta)$ means a Fourier transformation of $I(X,Y)$. The cross-correlation analysis is mainly applied to the analysis of microscope images in comparison with the phase variation in holography. By using the postsignal process, we assess the drying process of paints.

3 Experimental Configuration for the Combined Method

Experimental configuration of the combined holographic and gravimetric method for implementing the direct comparison between holographic signal and weight change of the specimen is illustrated in Fig. 1. A commercial water-based paint was applied to a copper (Cu) plate whose surface was parallel to the horizontal $x-y$ plane as shown in Fig. 1(a). The beam of a laser diode (LD) with 658 nm wavelength was expanded to a diameter of ~30 mm by a beam expander and used as the light source for the holographic method. The paint film was illuminated with the expanded laser beam after passing through a color filter F1 with a transmission band of 640 to 700 nm and beam splitters (BS1 and BS2).

The water-based paint was applied to the surface of the Cu plate of 40×40 mm^2 placed on an electronic balance with resolution of 0.1 mg. As shown in Fig. 1(b), a black paper sheet having an aperture of 20×20 mm^2 was placed on the Cu plate to avoid an aliasing effect in the hologram reconstruction. The paint was applied within the aperture using a paintbrush 6 mm wide. It is important to note that the paint is applied manually, so the reproducibility of films will be limited by the operator's skill; thus the global trends of the drying process are investigated. The samples were commercially available water-based paints for plastic models. One of them was a water-based acrylic resin paint whose color was silver (paint #1). The other was clear coat (transparent) and also a water-based acrylic resin paint (paint #2). The main ingredients of the paints provided by the manufacturer are listed in Tables 1 and 2, respectively.

To investigate a microscopic variation of pigment particles in paint #1, a microscope with a complementary metal oxide semiconductor (CMOS) camera was introduced into the setup as illustrated in Fig. 1(a). For the microscopic

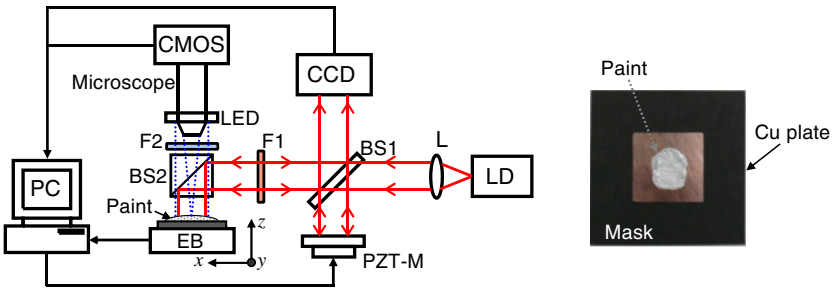

(a) Setup (b) Paint on the Cu plate

Fig. 1 Experimental configuration. (a), Setup. LD, laser diode; BS, beam splitter; F, color filter; PZT-M, piezo-transducer mirror; CCD, charge coupled device; CMOS, complementary metal oxide semiconductor; PC, personal computer; EB, electric balance. (b), Picture of the paint applied on the copper (Cu) plate.

observation, a blue-LED ($\lambda_c = 464$ nm) lighting system illuminated the paint film through another color filter F2 having a transmission band of 400 to 470 nm. The image in the microscope's field of view captured by the color CMOS camera with 1280×1024 pixels was sent to a personal computer (PC) via a USB interface. The microscope observed a central area of 0.69×0.55 mm^2 in the paint surface of paint #1 with magnification of ~700. The size of a pixel in the captured microscopic image corresponds to 0.54×0.54 μm^2. In the gravimetric measurement, the data of weight was sent to the PC via an RS-232C interface.

In the holographic observation, the diffusely reflected laser beam from the paint film was interfered with a reference beam reflected from a piezoelectric transducer (PZT: P.I. P-753.11C) mirror. Because the blue-light emitting diode (LED) light reflected from the film was blocked by the color filter F1, the interference pattern without the background LED light could be recorded by the CCD camera. After applying a stepwise phase shift of $\pi/2$ to the reference beam by the PZT mirror, four phase-shifting in-line holograms were captured by the CCD (Sony XC-66) camera of 512×512 pixels with 8-bit gray levels. The pixel size of the CCD was 12.87×12.92 μm^2. The exposure time of the CCD was 30 ms for each hologram recording, and the data acquisition for four phase-shifting holograms took 1 s. The video data were stored in a frame grabber (Cybertek CT-3000A) and sent to the PC for further analysis. The recording distances between the CCD and the paint surfaces were 546 mm for paint #1 and 537 mm for paint #2.

The hologram recording and the data acquisition of both weight and the microscopic image started after applying paint to the Cu plate. All the data acquisition was conducted with the interval of $T = 5$ s for a period of 2500 s. The measurements were performed in a closed box to reduce the influence of air flow and a change of environmental conditions. The experiment was conducted in a closed room in which the room temperature and humidity were almost constant during the measurement.

Table 1 Content of the main ingredients in the paint #1.

	Content (wt.%)	Evaporation rate (butyl acetate = 100)	Specific gravity (g/cm^3)
Isopropyl alcohol	20–30	150	0.786
Isobutyl alcohol	5–10	70	0.803
1-Methoxy-2-propanol	1–5	66	0.923
Water	10–30	38	1.0
Mineral spirit	1–5	20	0.791
2-Butoxyethanol	1–5	6	0.902
Pigment (Al)	~10	—	2.69
Acrylic resin	~20	—	—

Note: –, no data.

4 Results and Discussion

4.1 *Comparison between Digital Holographic and Microscopic Observations*

To study a time history of the reconstructed images and the microscope ones depending on the dryness of paint #1, the reconstructed intensity $I(X, Y; t)$ and phase difference

Table 2 Content of the main ingredients in the paint #2.

	Content (wt.%)	Evaporation rate (butyl acetate = 100)	Specific gravity (g/cm^3)	Refractive index
Ethanol	10–20	230	0.797	1.37
Isopropyl alcohol	20–30	150	0.786	1.38
Isobutyl alcohol	5–10	70	0.803	1.40
Water	10–30	38	1.0	1.33
2-Ethoxyethanol	4.9	32	0.931	1.41
2-Butoxyethanol	1–5	6	0.902	1.42
Acrylic resin	—	—	1.19	1.51

Note: —, no data.

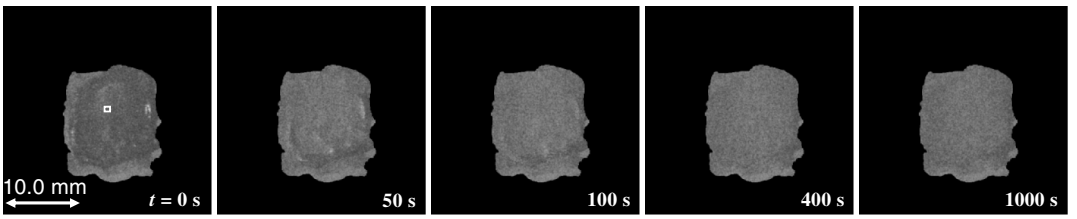

(a) Reconstructed intensity image $I(X,Y;t)$

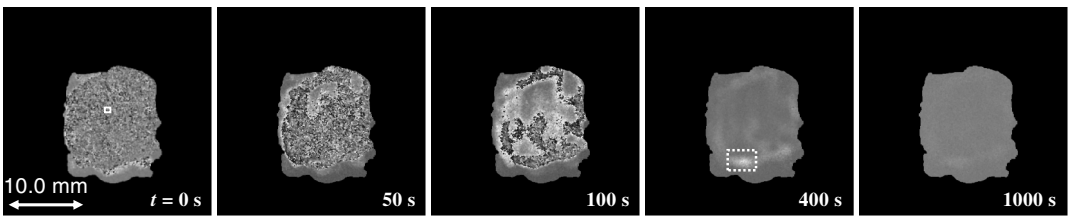

(b) Phase difference image $\Delta\phi\,(X,Y;t)$

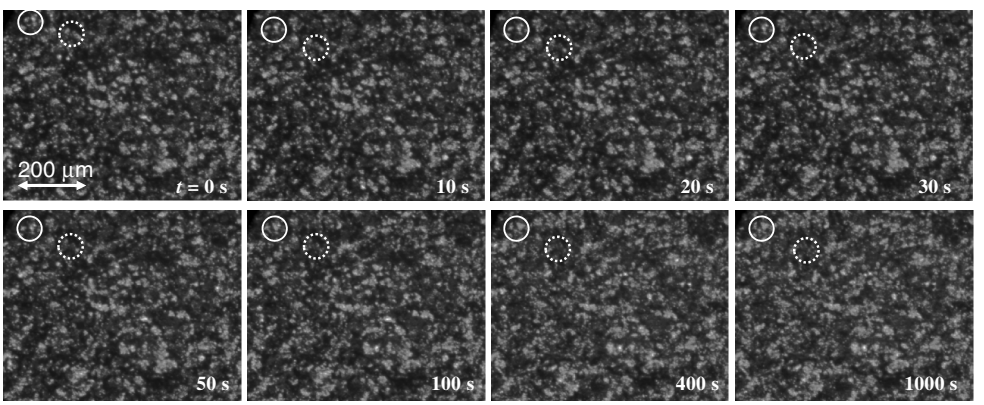

(c) Microscope image $I_m(X,Y;t)$

Fig. 2 Variation of images obtained for the paint #1 at different time lapses. (a), Reconstructed intensity image $I(X, Y; t)$. (b), Phase difference image $\Delta\phi(X, Y; t)$. (c), Microscopic images with magnification of 700. White rectangle (Area1) in (a) and (b) indicates the area observed with the microscope, and the dotted square (Area2) in (b) was analyzed for a local variation.

$\Delta\phi(X, Y; t)$ images at various lapses are shown in Fig. 2, together with the microscope images $I_m(X, Y; t)$. The measurement for paint #1 was conducted at a room temperature of 24.2°C and relative humidity of 51%. The dry thickness was about 19 μm, obtained by a micrometer caliper. To emphasize the variation occurring in the paint film, the original images of both $I(X, Y; t)$ and $\Delta\phi(X, Y; t)$ were multiplied by the intensity mask having a transmittance of 0 and 1. Therefore, these images in Fig. 2 represent only the painted area surrounded by the black area with the intensity or phase value being 0. The multiplication of the mask allows us to calculate the standard deviation σ_t in Eq. (3) within the painted area.

A white rectangle seen in both images of $I(X, Y; t)$ and $\Delta\phi(X, Y; t)$ at $t = 0$ s shows the area observed with the microscope. The size of the area (Area1) was 12×14 pixels (0.65×0.76 mm^2), approximately corresponding to the microscope field of view. To decrease the speckle noise caused by air flow and/or vibration, the phase difference was obtained after the conjugate product $U(X, Y; t)U^*(X, Y; t + T)$ was subjected to a moving average.[14] The size of the window for averaging was 3×3 pixels. The speckle noise seen in the phase differences $\Delta\phi(X, Y; t)$ can be effectively reduced by the filtering process.[14] The filtering process was also applied to the results for paint #2.

After the application of paint #1 with the paintbrush, a drying area expected from constant brightness expands as time passes in Fig. 2(b). As expected from the previously reported results for the solvent-based paint,[9,10] the time history of the phase difference $\Delta\phi(X, Y; t)$ can nicely represent a local variation of the dryness of the water-based paint as well. In the phase difference image at 400 s in Fig. 2(b), the dotted rectangle of 50×70 pixels (2.73×3.80 mm^2) shows the slowest drying region in the paint film. Figure 2(c) shows the variation of microscope images corresponding to the white square shown in both Fig. 2(a) and 2(b). The colors of the microscope images were converted into 8-bit gray scale. As seen in these images, the size of pigments is larger than 10 μm . In the first three images ($t = 0 \sim 20$ s), the movement of pigment particles can be perceived (e.g., in the white circles). After 100 s, no significant deformation in the distribution of pigment particles was observed.

The direct comparison between the holographic detection and microscopic observation can be achieved using the configuration in Fig. 1. The peak value C_{pm} of cross-correlation function $C(X, Y; t)$ in Eq. (6) for the two subsequent

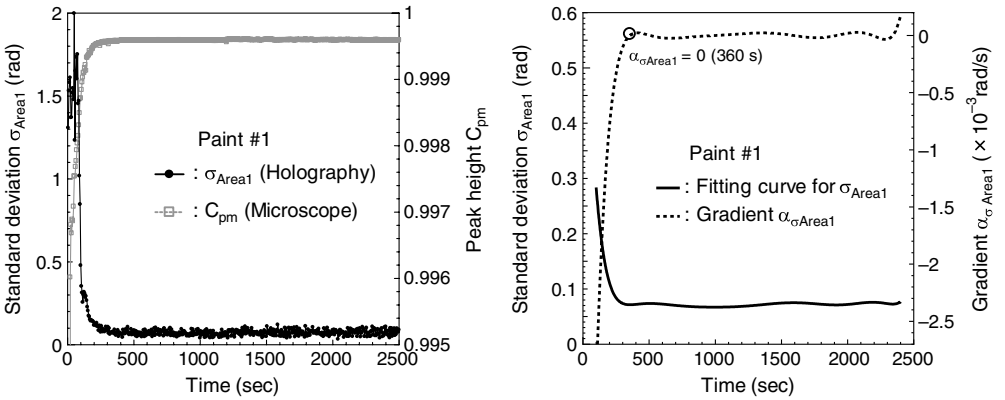

(a) C_{pm} and σ_{Area1} (b) σ_{Area1} and $\alpha_{\sigma Area1}$

Fig. 3 Comparison between microscopic observation and holographic analysis. (a), Peak value C_{pm} of cross-correlation function for two subsequent microscope images and the standard deviation σ_{Areal} of phase difference within Area1 obtained by holography. (b), Polynomial fitting curve for σ_{Areal} and a gradient $\alpha_{\sigma Areal}$ of the fitting curve.

microscope images and the standard deviation σ_{Area1} of the phase difference $\Delta\phi(X, Y; t)$ in Area1 were calculated as shown in Fig. 3. Because the structure of pigment particles in the microscope images shows no significant change as seen in Fig. 2(c), the value of C_{pm} becomes higher than 0.995. The variations of both the values of C_{pm} and σ_{Area1} converge simultaneously at around 350 s as seen in Fig. 3(a). It is found that the sensitivity of the phase obtained by the holographic method to a variation of the paint surface is almost the same as that of the microscope observation with magnification of 700. Therefore, the holographic method can analyze the paint surface of much larger area than the microscope's field of view with almost the same sensitivity as the microscope.

To determine a stationary state[10] of the paint surface within Area1 using the phase change σ_{Area1}, a polynomial fit to the variation of σ_{Area1} in Fig. 3(a) has been applied instead of the moving standard deviation in the past work.[10] The resultant fitting curve is shown in Fig. 3(b) with its gradient $a_{\sigma Area1}$. The stationary state of the paint surface within Area1 at which the gradient $\alpha_{\sigma Area1}$ becomes 0 can be estimated as 360 s. As expected from the time history shown in Fig. 2(b), it is reasonable that the painted surface within Area1 dried earlier than the other areas.

4.2 *Direct Comparison between Phase Change and Weight Loss of Paint #1*

The time history of the paint surface is analyzed quantitatively by calculating the cross-correlation function $C(X, Y; t)$ and the standard deviation σ of the phase difference $\Delta\phi(X, Y; t)$ in both the whole painted area and the slowest drying region (Area2) within the dotted rectangle in Fig. 2(b). Before the calculations, the reconstructed intensity was subjected to a moving average with a 3×3 matrix for a noise reduction. The results are compared directly with the variation of weight of paint M_p in Fig. 4.

In the constant rate period from $t = 0$ s to 140 s, the weight M_p decreases at the rate of 2.5×10^{-2} mg/s as shown in Fig. 4(a).[3] Enough solvent can maintain some separation of pigment particles, and thus the pigments showed relatively large movements as observed in the microscopic images of Fig. 2(c). In the period, the object light reaching at the CCD consists of the backscattered light from both the paint surface and the inside of the paint film. In the latter case, the light undergoes multiple scattering.[15] Thus, the large movement of pigment particles in the period causes the significant and rapid change in the wavefront of the object wave represented by σ as seen in Fig. 4(b).

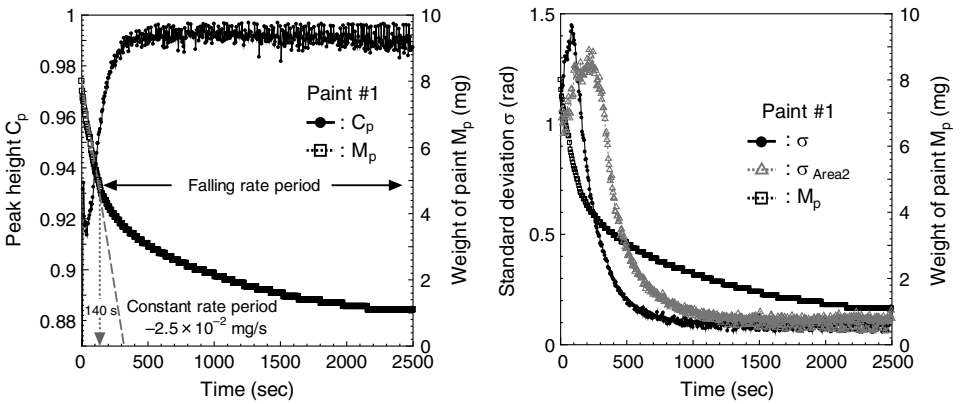

(a) C_p and M_p (b) σ and M_p

Fig. 4 Time dependence of C (a) and σ (b) calculated from the reconstructed complex amplitudes of the whole painted area and weight of paint M_p. σ_{Area2} is obtained from Area2 in Fig. 2(b).

The value of σ has increased for 200 s and then decreases monotonically. The behavior of σ is different from the speckle rate in the dynamic speckle method, in which the speckle rate decreases monotonically with time.[3,4,6] The difference in the behaviors is probably due to the sampling rate of data acquisition. The interval of 5 s in our method might be too long to follow the rapid variation due to the multiple scattering in the paint film just after the paint application. In the constant rate period, isopropyl alcohol and isobutyl alcohol have mainly evaporated because of their higher evaporation rate than the other solvents in the paint film as listed in Table 1.

After the constant rate period, a falling rate period with decreasing weight loss of the paint appears in the drying process as seen in the curve of M_p. In the falling-rate period, the pigment particles and acrylic resin in the paint film begin to appear at the surface due to the evaporation of solvents. Therefore, the object light mainly consists of the backscattered light from the paint surface. A drastic decrease in the movement of pigment particles leads to a reduction of change in the reflected wave from the paint surface as seen in both Fig. 4(a) and 4(b). The phase change in the whole painted area represented by σ reaches a plateau at around 1000 s before the weight of paint M_p. This is because the value of σ in the falling rate period represents mainly the movement of paint surface, whereas the weight M_p represents the evaporation of the solvent in the whole paint film.

For the detection of the stationary state of the paint film, a polynomial fit has been applied to both curves of σ and σ_{Area2} in Fig. 4(b). Figure 5 shows the resultant fitting curves for both σ and σ_{Area2} together with their gradient ones. The stationary state of the whole painted area at which the phase change stops with $\alpha_\sigma = 0$ can be obtained as 1230 s. In the same way, it is found that the phase change within Area2 converges at 1750 s. This discrepancy in time between two stationary states is due to both a negligibly small contribution of Area2 to a whole painted area and a very low signal-to-noise ratio for the phase change σ after 1000 s. Thus, some weight loss ΔM_p after 1230 s is due to the evaporation from undried small areas such as Area2. From the confirmations by touching the painted surface

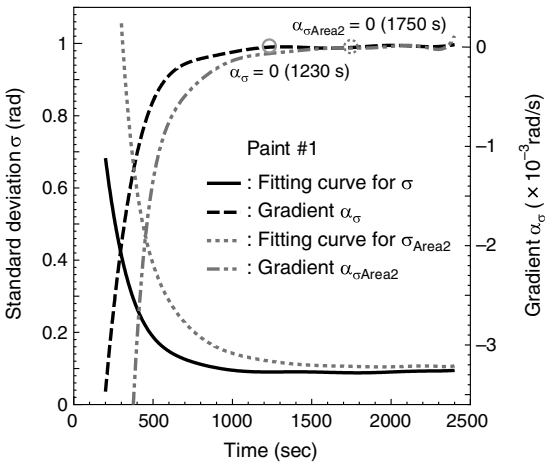

Fig. 5 Fitting curves for the standard deviations σ and σ_{Area2} obtained, respectively, from the whole painted area and Area2 in the period of 200 to 2500 s in Fig. 4(b) and their gradients α_σ calculated from the curves.

for paint #1, a tack-free state has been usually obtained at around 550 to 700 s under the condition of temperature 15°C to 26°C and relative humidity 45% to 66%. Thus, the stationary state obtained at 1230 s possibly corresponds to a state of dry-hard of paint #1 except for the undried Area2.

Figure 6(a) shows the temporal variation of weight M_p and weight loss ΔM_p of paint #1. As seen in Fig. 6(a), the content of solvents in paint #1 is estimated to be ~86 wt.%. To investigate the variation of weight loss, the polynomial fit is applied to the curve of M_p, and its gradient is calculated as shown in Fig. 6(b). The rate of weight loss for paint #1 after 1230 s has decreased to about 1.0×10^{-3} mg/s, which becomes less than one twentieth of that in the constant-rate period. At 1750 s, most solvents in the paint film have evaporated and the amount of residual solvents is estimated to be 0.3 mg from Fig. 6(a). It is presumed that the residual solvents mainly consist of mineral spirit and 2-butoxyethanol in Table 1 because of their low evaporation rate.

By comparing the phase change and the weight loss simultaneously, a relationship between solvent evaporation and surface activities of the paint film can be adequately analyzed to estimate the mechanism of the drying process.

4.3 *Monitoring of Dryness and Analysis of Solvent Evaporation for Paint #2*

A drying process of clear coat has also been investigated using paint #2. Because paint #2 has no pigment particles acting as scatterer for the incident laser light and is transparent in the visible light region, no dynamic speckle arising from the light-scattering by surface activity of paint film may be expected. In the proposed method, the phase change of the reconstructed object wave due to a variation of paint thickness can be used to monitor the drying process of paint #2. The measurement for paint #2 was conducted at a room temperature of 18.6°C and relative humidity of 38%. The dry thickness of paint #2 was about 21 μm.

In the reconstructed images, only phase difference distribution $\Delta\phi(X,Y;t)$ can show a clear temporal variation in the drying process. Figure 7 shows the temporal variation of phase difference images $\Delta\phi(X,Y;t)$. These images also show only the painted area using the intensity mask described in the analysis for paint #1. Because the Cu plate in Fig. 1 has a surface smooth enough to specularly reflect the incident laser light, the phase difference image $\Delta\phi(X,Y;t)$ shows a pattern due to the variation of optical pathlength resulting from both a reduction of paint thickness and a refractive index change. Main solvents included in paint #2 are ethanol, isopropyl alcohol, isobutyl alcohol, and water as listed in Table 2. The refractive index of these solvents ranges from 1.33 to 1.42, and that of acrylic resin is around 1.51.[3] Therefore, no significant changes in the refractive index of paint film are expected when solvents evaporate from the film coating during the interval of 5 s. The effect of multiple scattering due to nonuniform refractive index seems to be negligibly small.[15] By virtue of the filtering process for the conjugate product $U(X,Y;t)U^*(X,Y;t+T)$, the speckle noise can be effectively removed. Thus, the temporal variation of $\Delta\phi(X,Y;t)$ after the noise filtering mostly represents the change of film thickness. In other words, these images

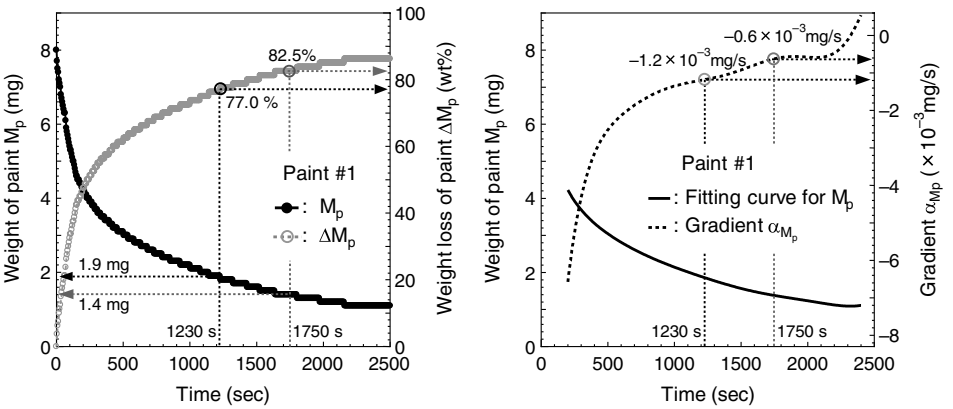

Fig. 6 Variation of weight of the paint M_p and a fitting curve for M_p and the gradient α_{Mp} of the fitting curve. Weight of paint #1 is measured with the electric balance with a resolution of 0.1 mg.

show the deformation of paint film and equivalently dryness of paint #2.

In an early drying process from 0 to 120 s in Fig. 7, local deformations observed in $t = 0$ s gradually merge into a concentric variation as seen in a central area of the image at 120 s. The change of the pattern in the early drying process is associated with the leveling of paint #2.[11] A deformation around the edge of the paint film seen at 400 s fades out before 1000 s. These local variations seen in the phase-difference images show a process of leveling and film formation in the drying of clear coat.

The same data processing for the phase difference $\Delta\phi(X, Y; t)$ as that for paint #1 has been applied to the analysis of the variations in Fig. 7. Figures 8 and 9 show the results for both the standard deviation σ and weight of paint M_p. The stationary state of paint #2 for the criteria $\alpha_\sigma = 0$ is obtained as 1060 s, which corresponds to the completion of film deformation. The amount of residual solvents at 1060 s can be estimated to be more than 0.4 mg from Fig. 9. The weight loss ΔM_p due to solvent evaporation continues after the stationary state. The rate of weight loss for paint #2 at 1060 s is 0.75×10^{-3} mg/s, which is almost the same as the value obtained for paint #1 at the stationary state. In the last stage of the falling-rate period, the contribution of evaporation to the phase change seems to be very small and buried in environmental noise such as vibration and/or air flow.

The tack-free state of paint #2 has usually been obtained at around 650 to 750 s under the conditions of temperature 16°C to 17°C and relative humidity 46% to 51%. Thus, the stationary state at 1060 s possibly corresponds to a state of dry-hard of paint #2. In Fig. 9, the content of solvents in paint #2 is estimated to be ~73 wt.%. As shown in both Figs. 7 and 8, it is possible that the drying process of clear coat including no pigment particles can also be visualized and numerically investigated by the proposed method.

To further investigate the temporal film deformation, the phase-difference patterns in Fig. 7 are unwrapped; the unwrapped images in grayscale are shown in Fig. 10. The brightness of the image represents a magnitude of deformation, in this case, a decrease in film thickness. At the beginning, a local deformation due to nonuniformity in the film thickness can be seen as expected in wrapped phase patterns in Fig. 7. The deformation gradually decreases with time. Figure 11 shows the variation along the dotted lines in Fig. 10. The negative values of phase change seen in Fig. 11(a) and 11(b) mean an increase in film thickness. This phenomenon due to film leveling can be seen within

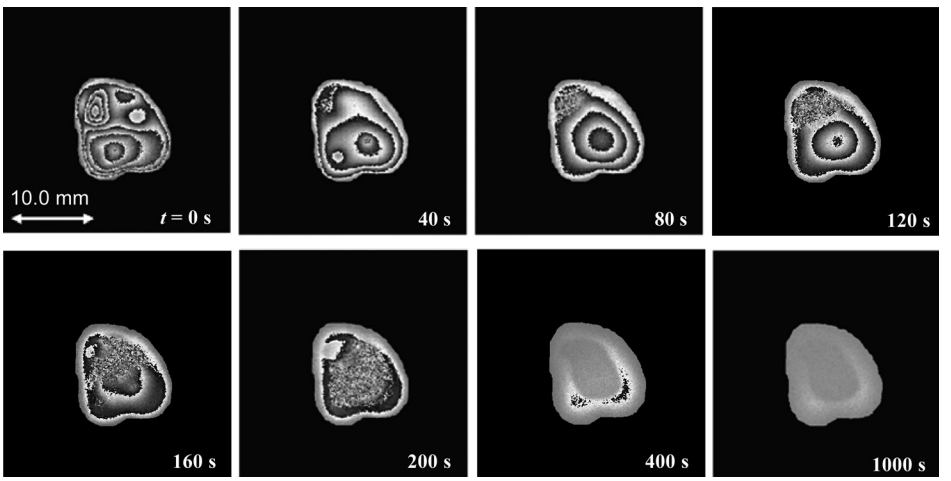

Fig. 7 Variation of phase difference images $\Delta\phi(X, Y; t)$ obtained for paint #2 at different time lapses.

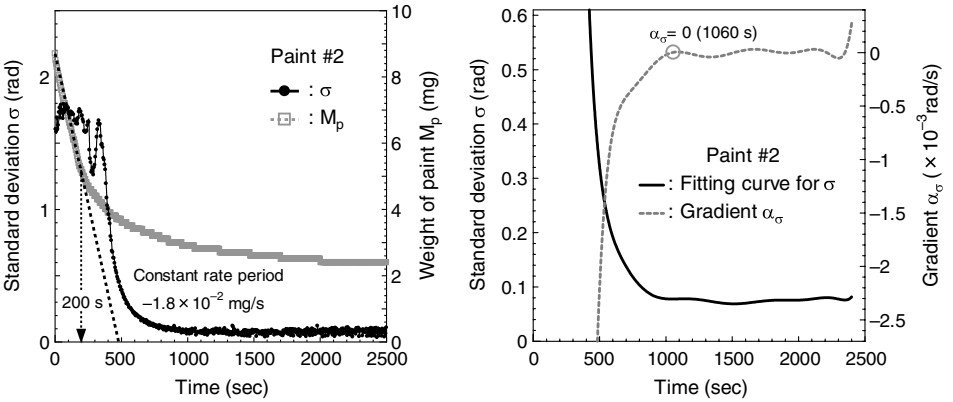

Fig. 8 (a), Time dependence of a standard deviation of the phase difference σ calculated from the reconstructed complex amplitudes and weight of paint #2 M_p. (b), Time dependence of a fitting curve to the values of σ and its gradient α_σ obtained for paint #2.

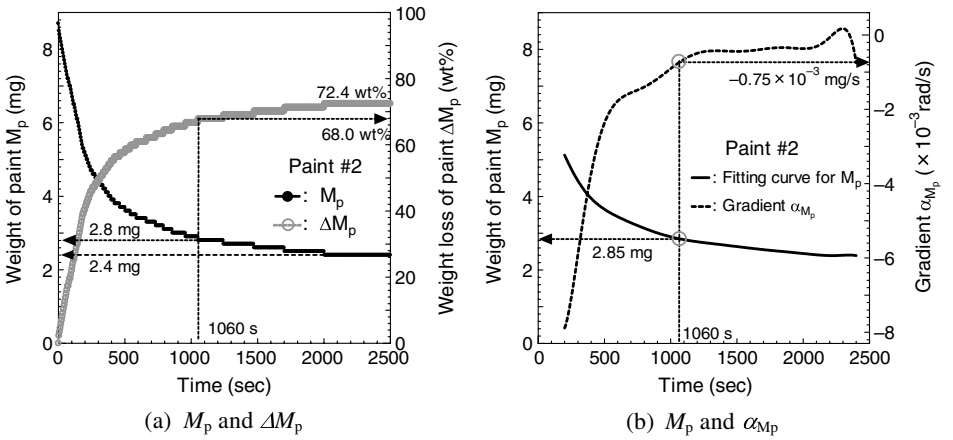

Fig. 9 Variation of weight of paint #2. (a), Weight M_p and weight loss ΔM_p. (b), A fitting curve to M_p and a gradient of the fitting curve α_{Mp}.

a few tens of seconds after paint application. After 300 s, the phase change converges because of the decrease of film thickness due to the evaporation of solvents.

To estimate the volume of evaporating solvent, the refractive index n_{film} of the paint film is estimated using the component ratio in Table 2 and the residual weight in Fig. 9. The weight of paint #2 at 2500 s is 2.4 mg, corresponding to 27.6 wt.% of the initial weight 8.7 mg. Because the paint film is not completely dried at 2500 s, the content of acrylic resin can be roughly estimated as 25 wt.%. On the assumption that the initial content of solvents in the paint film was 75 wt.% and then the paint film consisted of 75% of the maximum value for each solvent in Table 2, the initial refractive index of the paint film is estimated as 1.395. In the assumption, the local distribution of refractive index is not taken into account. Then, the decreased volume Δv of paint film due to solvent evaporation can be calculated using Eqs. (4) and (5) if the refractive index of the paint film was constant. The specific gravity d_e of evaporating solvent for each time is also obtained by dividing the temporal weight loss ΔM_p by the volume Δv as shown in Fig. 12.

Excepting the first 50 s, the value of d_e varies between 0.85 and 0.95 g/cm^3 during the first 200 s. Ethanol and/or isopropyl alcohol evaporate mainly in the early stage because of their high evaporation rate as seen in Table 2. Though the value of d_e becomes a bit larger than those for the alcohols in Table 2, the results agree roughly with

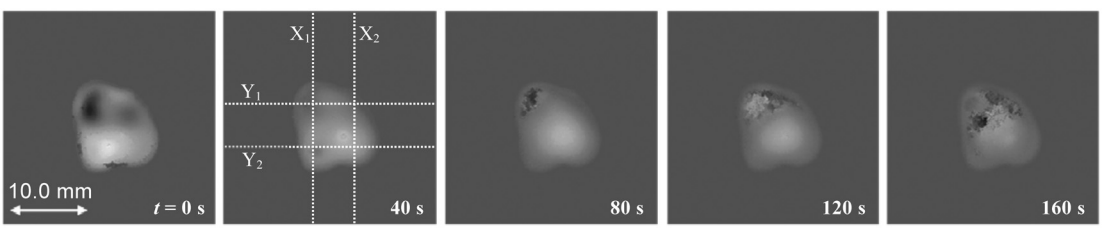

Fig. 10 Variation of phase-unwrapped images in Fig. 7 at different time lapses.

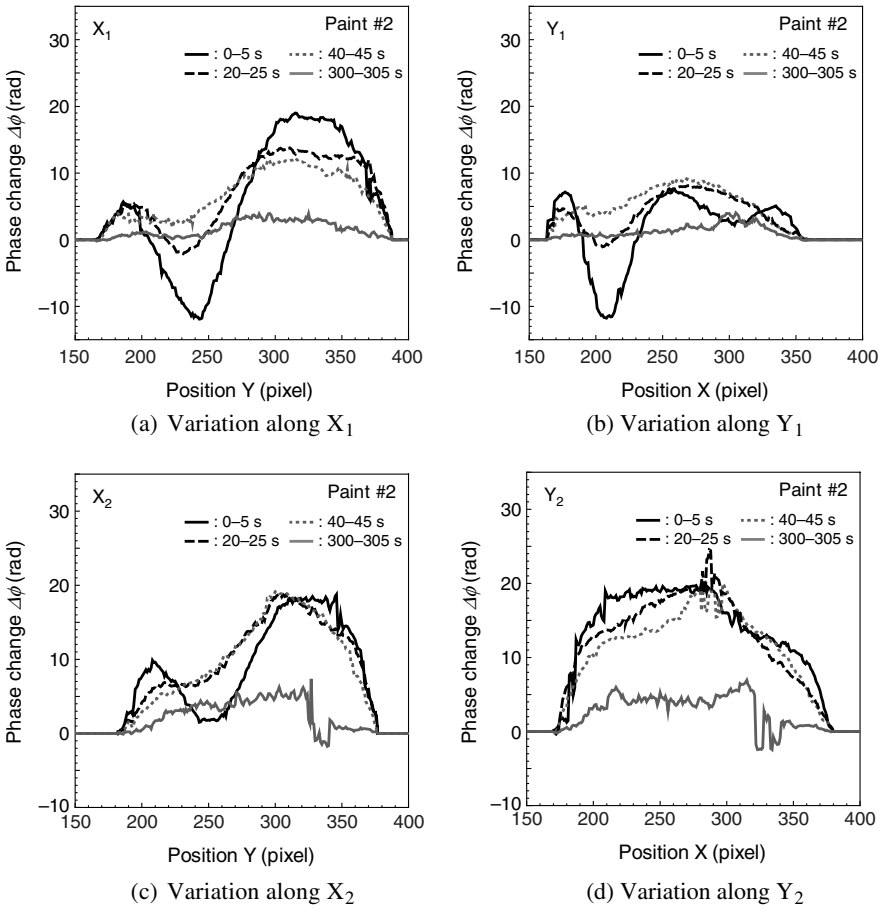

Fig. 11 Cross-sectional variation of phase change along each dotted line in Fig. 10. (a) and (c) are along X_1 and X_2, respectively, (b) and (d) are along Y_1 and Y_2, respectively.

the specific gravity of the alcohols. The large discrepancy seen in the first 50 s may be due to an underestimation of the phase change arising from the multiple reflections in the paint film and/or the slow data sampling of 5 s. After 200 s, the value of d_e fluctuates around 1.0 g/cm^3 and then increases gradually up to 1.1 g/cm^3. The refractive index of the paint film actually increases up to that of acrylic resin owing to the evaporation of solvents. When the increasing refractive index up to 1.51 is taken into account, the value of d_e is probably corrected to around 1.0 mg/cm^3, corresponding to the value of the lower three solvents in Table 2. The temporal variation of d_e roughly represents the global trend of solvent evaporation. Therefore, the dependence of film formation for clear coat on the composition of solvents might be investigated using the method.

For further investigation of film formation, it may be possible to apply a photoelastic analysis to the paint film using the orthogonal polarized reference waves in digital holography.[16,17]

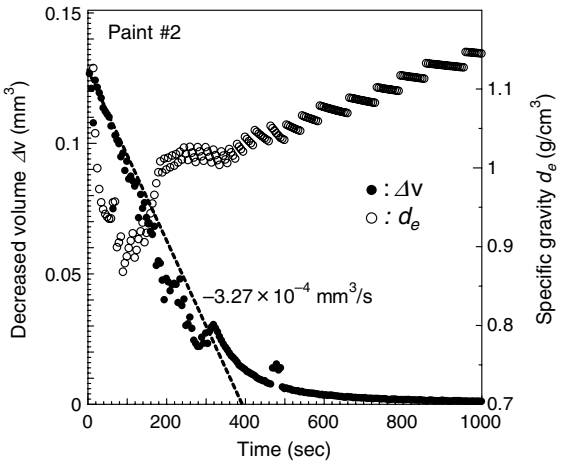

Fig. 12 Time dependence of a volume reduction in the paint film obtained from the value of phase change $\Delta\phi$ in Fig. 10 and the specific gravity d_e of evaporated solvent estimated using the values of both Δv and M_p in Fig. 9.

5 Conclusions

We have demonstrated a novel method combining digital holography and gravimetric measurement to fulfill the direct comparison for the further assessment of the paint drying process. The results indicate that the present technique has high sensitivity to surface variations, allowing us to investigate the drying process of paints, including clear coat having no pigment particles. In addition, it has been shown that the sensitivity of phase to the surface change in the holographic method is estimated to be the same level as the microscope observation.

Using both the new approach for detecting a stationary state and the simultaneous observation with the gravimetric

measurement, we can investigate the relationship between the phase variation occurring in the paint film and the evaporation of solvent from the film. In addition, the specific gravity of solvents in the clear coat is also estimated using both the reduced volume obtained from the phase change and weight loss of the paint film. The estimation of specific gravity may be highly useful for the determination of base material in paints. From these results, it is shown that the proposed combined method is highly useful for the investigation of drying process up to dry-hard state of paints even though the sample is clear coat. For further investigation, the information of polarization may be useful for assessment of the film formation of clear coat, and one-shot phase-shifting digital holography is also helpful for an observation of rapid variation in drying process.[18,19]

References

1. S. Croll, "Dyring of latex paint," *J. Coat. Technol.* **58**(734), 41–49 (1986).
2. G. Romero, E. Alanis, and H. Rabal, "Statistics of the dynamic speckle produced by a rotating diffuser and its application to the assessment of paint drying," *Opt. Eng.* **39**(6), 1652–1658 (2000).
3. J. Amalvy et al., "Application of dynamic speckle interferometry to the drying of coatings," *Prog. Org. Coat.* **42**(1–2), 89–99 (2001).
4. A. Brun, L. Brunel, and P. Snabre, "Adaptive speckle imaging interferometry (ASII): new technology for advanced drying analysis of coatings," *Surf. Coat. Int. B Coat. Trans.* **89**(B3), 193–268 (2006).
5. R. Arizaga et al., "Following the drying of spray paints using space and time contrast of dynamic speckle," *JCT Res.* **3**(4), 295–299 (2006).
6. P. Faccia et al., "Differentiation of the drying time of paints by dynamic speckle interferometry," *Prog. Org. Coat.* **64**(4), 350–355 (2009).
7. I. Yamaguchi et al., "Monitoring of paint drying process by digital speckle correlation," *Opt. Rev.* **14**(6), 362–364 (2007).
8. G. Sheoran, S. Sharma, and C. Shakher, "Monitoring of drying process and cracking/disbanding of paints using lensless Fourier transform digital holography," *Opt. Laser Eng.* **49**(1), 159–166 (2011).
9. M. Yokota, T. Adachi, and I. Yamaguchi, "Monitoring and evaluation of drying of paint by using phase-shifting digital holography," *Opt. Eng.* **49**(1), 015801 (2010).
10. M. Yokota et al., "Drying process in a solvent-based paint analyzed by phase-shifting digital holography and an estimation of time for tack free," *Appl. Opt.* **50**(30), 5834–5841 (2011).
11. A. Quach, "Polymer coatings. physics and mechanics of leveling," *Ind. Eng. Chem. Prod. Res. Develop.* **12**(2), 110–116 (1973).
12. I. Yamaguchi and T. Zhang, "Phase-shifting digital holography," *Opt. Lett.* **22**(16), 1268–1270 (1997).
13. U. Schnars and W. Juptner, "Direct recording of holograms by a CCD target and numerical reconstruction," *Appl. Opt.* **33**(2), 179–181 (1994).
14. I. Yamaguchi and M. Yokota, "Speckle noise suppression in measurement by phase-shifting digital holography," *Opt. Eng.* **48**(8), 085602 (2009).
15. L. Le Hors et al., "Phenomenological model of paints for multispectral polarimetric imaging," *Proc. SPIE* **4370**, 94–105 (2001).
16. M. Yokota, Y. Terui, and I. Yamaguchi, "Polarization analysis with digital holography by use of polarization modulation for single reference beam," *Opt. Eng.* **46**(5), 055801 (2007).
17. M. Yokota, "Polarization analysis by off-axis digital holography with an improved optical system and an evaluation of its performance by simulation," *Appl. Opt.* **47**(34), 6325–6333 (2008).
18. T. Nomura and M. Imbe, "Single-exposure phase-shifting digital holography using a random-phase reference wave," *Opt. Lett.* **35**(13), 2281–2283 (2010).
19. Y. Awatsuji et al., "Parallel optical-path-length-shifting digital holography," *Appl. Opt.* **48**(34), H160–H167 (2009).

Masayuki Yokota received the BS, MS, and PhD degrees in electronic engineering from Gunma University in 1989, 1991, and 1998, respectively. Currently, he is an associate professor at the Department of Electronic and Control Systems Engineering, Shimane University, where he has been working on optical engineering. His research interests include interferometry, holography, optical fiber sensors, and optical information processing. He is a member of the Japan Society of Applied Physics (JSAP), the Optical Society of Japan (OSJ), the International Society of Optical Engineering (SPIE), and the Optical Society of America (OSA).

Yoshiki Kimoto received the BS degree in electronic and control systems engineering from Shimane University in 2010. Currently, he is a MS student at Department of Electronic and Control Systems Engineering, Shimane University.